Environmental Science Nano

Toxicity of Single-Walled Carbon Nanotubes (SWCNTs): Effect of Lengths, Functional Groups and Electronic Structures Revealed by a Quantitative Toxicogenomics Assay

Journal:	*Environmental Science: Nano*
Manuscript ID	EN-ART-03-2020-000230.R1
Article Type:	Paper

Environmental significance statement: (~ 3-5 sentences)

The blooming rate in the production and application of CNTs in various fields has prompted accompanying rise in public concerns on the possible toxicological risks and implications related to these CNMs. Systematic studies of the relationship between the toxicological effects and mechanisms of SWCNTs and their physicochemical properties are still scarce in the literature and thus are greatly needed. This study quantitatively compared the cellular toxicity profiles and mechanisms among 6 SWCNTs with varying length, functional groups and electronic structures with the object to elucidate the toxicological effects of SWCNTs and their dependence on physicochemical properties. The results contribute to the advancement of our mechanistic understanding of SWCNT nanotoxicity based on their fundamental properties, which will provide a scientific basis for CNM regulatory management and risk mitigation.

Toxicity of Single-Walled Carbon Nanotubes (SWCNTs): Effect of Lengths, Functional Groups and Electronic Structures Revealed by a Quantitative Toxicogenomics Assay

Tao Jiang[1], Carlo Alberto Amadei[2], Na Gou[1,4], Yishan Lin[1,4], Jiaqi Lan [1,3], Chad D. Vecitis[3], April Z. Gu[4*]*

1. Department of Civil and Environmental Engineering, Northeastern University, 360 Huntington Ave, Boston, MA 02115

2. John A. Paulson School of Engineering and Applied Sciences, Harvard University, Cambridge, MA 02138

3. Institute of Materia Medica, Chinese Academy of Medical Sciences and Peking Union Medical College, Beijing, 100050, China

4. School of Civil and Environmental Engineering, Cornell University, 220 Hollister Dr., Ithaca, NY 14853

* Corresponding authors: aprilgu@cornell.edu, gracelanjiaqi@gmail.com

Abstract (50-250 words)

Single-walled carbon nanotubes (SWCNTs) are a group of widely used carbon-based nanomaterials (CNMs) with various applications, which raise increasing public concerns associated with their potential toxicological effect and risks on human and ecosystems. In this report, we comprehensively evaluated the nanotoxicity of SWCNTs with their relationship to varying lengths, functional groups and electronic structures, by employing both newly established quantitative toxicogenomics test, as well as conventional phenotypic bioassays. The objective is to reveal potential cellular toxicity and mechanisms of SWCNTs at the molecular level, and to probe their potential relationships with their morphological, surface, and electronic properties. The results indicated that DNA damage and oxidative stress were the dominant mechanisms of action for all SWCNTs and, the toxicity level and characteristics varied with length, surface functionalization and electronic structure. Distinguishable molecular toxicity fingerprints were revealed for the two SWCNTs with varying length, with short SWCNT exhibiting higher toxicity level than the long one. In terms of surface properties, SWCNT functionalization, namely carboxylation and hydroxylation, led to elevated overall toxicity, especially genotoxicity, as compared to unmodified SWCNT. Carboxylated SWCNT induced a greater toxicity than the hydroxylated SWCNT. The nucleus is likely the primary target site for long, short, and carboxylated SWCNTs and mechanical perturbation is likely responsible for the DNA damage, specifically related to degradation of the DNA double helix structure. Finally, dramatically different electronic structure-dependent toxicity was observed with metallic SWCNT exerting much higher toxicity than the semiconducting one that exhibited minimal toxicity among all SWCNTs.

Key Words: carbon-based nanomaterials (CNMs), single-walled carbon nanotubes (SWCNTs), nanotoxicity, genotoxicity, oxidative stress, quantitative toxicogenomics assay, comet assay, reactive oxygen species (ROS)

Introduction

Carbon nanotubes (CNT) are a broadly utilized group of carbon-based nanomaterials (CNMs) due to their unique mechanical, optical, electrical and thermal properties. The hollow CNTs are divided into single-walled carbon nanotubes (SWCNT) and multi-walled carbon nanotubes (MWCNT). There has been tremendous enthusiasm in exploring the exemplary CNT properties for various bioengineering applications, including biosensors and biodevices for identification of biomolecules and cells [1-3], delivery of drugs and vaccines [4-6], tissue bioengineering [7, 8], and neuronal growth [9, 10].

The blooming rate in the production and application of CNTs in various fields has prompted accompanying rise in public concerns on the possible toxicological risks and implications related to these CNMs. Due to the difficulty in determining the accurate CNT concentrations in real environmental matrices [11, 12], modeling approaches have estimated the expected CNT concentrations in the aquatic environment and sediments to be in the range of ng/L to perhaps low μg/g based on estimates of production, disposal, and persistence [13-15]. Although the risk of CNT bioaccumulation in the environment is considered to be low [16, 17], laboratory studies have demonstrated that CNTs may be accumulated by both plants and animals [18, 19]. Petersen et al. have reported that the water flea *Daphnia magna* can accumulate CNTs in its gut, although the absorption into cellular tissues was unobservable [20, 21].

Due to their fiber-like structure, CNT could stimulate asbestos-like pathology, e.g. oxidative stress as well as pulmonary and inflammatory effects [22-25]. CNT-induced effects observed in humans, mice, rats and many other species have been associated with cytotoxicity [26-28], genotoxicity [29-31], epigenetic toxicity [32], splenic toxicity [33], immunotoxcity [34, 35], dermal and eye irritation and skin sensitization [36], inhibition of lactate dehydrogenase activity [37] as well as fecundity and growth [38]. CNT toxicity has been recognized to be influenced by various factors such as material preparation, surface properties, and characterization methodologies, which have resulted in seemingly inconsistent and even contradictory observations [39-41].

The toxicity of single-walled carbon nanotubes (SWCNTs) could be affected by a wide range of morphological, surface, and electronic properties [42-46]. Most previous studies on SWCNT toxicity have focused on a single or few properties and features each time. Moreover, most studies focused on specific phenotypic endpoints, and molecular level mechanisms were relatively rare. It is of great significance to develop a comprehensive mechanistic understanding of SWCNT nanotoxicity based on their fundamental properties, which will provide a scientific basis for CNM regulatory management and risk mitigation. In summary, systematic studies of the relationship between the toxicological effects and mechanisms of SWCNTs and their physicochemical properties are still scarce in the literature [47] and thus are greatly needed.

Most nanotoxicity studies have employed conventional animal-based, e.g. mice and rats, phenotypic toxicity assessment methods due to their anatomical similarities to human health issues [25, 48-50]. However, the resource-intensiveness, sophisticated analytical methodology, and long testing periods associated with animal-based experiments make it

very challenging, if even possible at all, to evaluate the large and ever increasing number and diversity of nanomaterials [51]. Therefore, a systematic transition from animal-based tests to a tiered screening and evaluation system that incorporates high throughput, mechanistic nanotoxicity testing methodologies and predictive toxicological models is urgently needed [51-53].

Recently, we have developed and demonstrated a novel toxicogenomics-based high-throughput 3-dimensional (exposure time, specific protein, expression alteration magnitude) differential protein expression profiling technique, using GFP-fused yeast reporter arrays, for fast, effective and mechanistic toxicity assessment [31, 54]. In addition, we have developed the Protein Expression Level Index (PELI) for determination of quantitative toxicogenomics endpoints [31, 55-57]. We have demonstrated successful application of this technology for comparing and evaluating genotoxicity potential and mechanisms among various NMs [31]. Additionally, a variety of researchers have demonstrated the successful application of genomics [58], as well as other omics technologies such as proteomics [59-63] and metabonomics [64-66] for SWCNT toxicity evaluation.

In this study, we comprehensively assessed the nanotoxicity of SWCNTs with different lengths, surface groups, and electronic structures by employing the newly established quantitative toxicogenomics-based toxicity assay as well as by conventional phenotypic bioassays. In addition, detailed and comprehensive characterization of the SWCNTs of varying properties were performed. The results elucidated the SWCNT structure-dependent toxicology and revealed the relationship between the observed toxicity mechanisms and SWCNT physicochemical properties.

2. Materials and Methods

2.1 Nanomaterials Information and Preparation

Six different types of single-walled carbon nanotubes (SWCNTs), including two SWCNT with different lengths (unmodified SWCNTs; 0.5-2 and 5-30 μm; purity > 90%; Cheap Tubes Inc., VT, USA), two with different functional groups (carboxyl and hydroxyl; purity > 90%; Cheap Tubes Inc., VT, USA), and two with different electronic states (metallic and semiconducting; purity > 98%; NanoIntegris, IL, USA), were assessed in this study (see detailed information in Table 1). The SWCNT characterization is provided in Section 2.2. The synthesis of unmodified and functionalized SWCNTs were through catalytic chemical vapor deposition, followed by purification using dilute nitric acid solution, containing < 3 wt% amorphous carbons and 5-6 wt% MWCNTs (product information from Cheap Tubes). The functionalization of SWCNTs was achieved by air oxidation. The metallic and semiconducting SWCNT were further purified by first heating to 300 °C in an oven for 4 h to remove amorphous carbon (Vecitis et al., ACS Nano, 2010). The SWCNT were then dispersed by bath sonication in concentrated HCl and heated to 60 °C overnight to remove any residual metals.

SWCNTs stock solutions were prepared as 20 times (640 mg/L) of the highest tested concentrations in phosphate buffered saline (PBS) using 1% bovine serum albumin (BSA; purchased from Acros, NJ, USA) as the dispersant which is commonly used in nanotoxicity bioassays [63, 67]. The stock solutions were sonicated using a bath sonicator at ~130 watt or 15 min to obtain a good dispersion, immediately followed by dilution in synthetic defined (SD) medium for subsequent tests.

The intention of this study is to perform hazard assessment that reveals the impact of various SWCNT properties on its molecular toxicity profiles and mechanisms, rather than to conduct environmental relevant risk analysis. Due to the ability of the toxicogenomics assay for capturing subtle molecular level responses, six sub-cytotoxic concentrations with 4-fold change (i.e. 32-0.031 mg/L for unmodified and functionalized SWCNTs, and 8-0.0078 mg/L for metallic and semiconducting SWCNTs), with the highest concentration as IC5 (inhibition concentration, 5%), were selected based on our previous nanotoxicity study [31].

2.2 Characterization of SWCNTs

The characterization of SWCNTs were performed using a Field Emission SEM (FE-SEM) with an in-lens secondary electron (Zeiss ULTRA, CA) for morphological observation, a transmission electron microscope (TEM) (Philips Tecnai F20) for examining the purity and defects in metallic and semiconducting nanotubes, and an X-ray photoelectron spectroscopy (XPS; Thermo Scientific, USA) for surface elemental composition analysis. The quantification of elemental compositions was performed by the Thermo Scientific Avantage software. The XPS instrumental error for elemental percentages was ± 0.1% [68]. Zeta potential, conductivity and aggregation sizes of SWCNTs in SD medium during exposure time of toxicogenomics assay (2 h) were examined by a dynamic light scattering (DLS) analyzer (Malvern Zetasizer Nano ZS90).

2.3 Toxicogenomics Assay and Quantitative Molecular Endpoint Derivation

The yeast biomarkers ensemble-based library was based on selected of cellular stress response pathways and biomarkers that are considered conserved across species. Yeast cells have commonly been used for toxicity studies because they share fundamental

strategies and defense responses to damage and stress with different eukaryotic cells [69-71], providing a promising basis for cross-species extrapolation commonly used in toxicity tests. Further, the yeast genome has been well studied, with substantial information available on gene function in public database (e.g. Saccharomyces Genome Database) and, through this, systematic cellular response pathways and molecular events occurring as a response to chemical exposure can be evaluated [72-74]. Yeast also offers several advantages over higher organisms, including being easy and fast to grow in unlimited quantities, ease of maintenance and storage, low cost, and rapid response.

The detailed description about the procedures of the toxicogenomics assay employing GFP-fused reporter yeast cells (*S. cerevisiae*) can be found in our previous reports [31, 55-57]. We used a library of 74 in frame GFP-fused proteins (SI Table S1) of yeast (Invitrogen, no. 95702, ATCC 201388) that were built through homologous recombination directed by oligonucleotide to label each ORF with *Aequrea victoria* (jellyfish) GFP in its chromosomal location at the 3' end [31, 75, 76]. The assay covers a wide range of key biomarkers indicative of all known important toxicological pathways of yeast in main stress categories, i.e. general, chemical, DNA, oxidative and protein stress [75, 77-79].

Briefly, yeast strains selected for toxicity assessment were incubated in clear-bottom black-wall 384-well plates with SD medium until the growth of cells reached the early exponential phase (with OD600 around 0.2-0.4). The 10 μL SWCNTs solution (pre-dissolved in PBS), along with blank control (SD medium + 0.25% YPD medium with or without SWCNTs), and internal control (SD medium + 0.25% YPD medium + PGK1 strain with or without SWCNTs), were added to plate wells to obtain the desired final

concentrations. PBS with 1% BSA was employed as the vehicle control. The yeast strain fused with housekeeping gene PGK1 was used as an internal control for plates normalization [55]. After adding the chemicals and controls, the plates were then monitored for cell growth (OD600 absorbance) and GFP signals of protein expression (485 nm excitation and 535 nm emission) by a microplate reader (Synergy H1 Multi-Mode, Biotech, Winooski, VT) for 2 h exposure at an interval of 5 min. All testing was conducted in dark in triplicate. Details of data processing for the yeast toxicogenomics assay can be found in the Electronic Supplementary Information (ESI).

For each SWCNT, PELI-based concentration-response patterns were modeled employing the Four Parameter Logistic (4PL) nonlinear regression model. Toxicity of positive or negative threshold value was set as PELI value of 1.5, which was determined based on the signal to noise ratio for the similar systems based on previous research and the standard deviation range in our toxicogenomics assay [31, 56]. The derivation of PELI-based molecular endpoint PELI1.5 (mg/L) was described in our previous studies [55, 57]. Additionally, genotoxicity and oxidative stress induced by each SWCNT at PELI1.5 was expressed as toxic equivalents geno-TEQ1.5 and oxi-TEQ1.5, respectively, for which mitomycin C (MMC) and H_2O_2 was employed as the reference compound, respectively [80, 81,49]. Since molecular weight is not available for SWCNTs, the unit mg/L was used in the equation.

2.4 Intracellular ROS Production Measurement

The intracellular ROS production induced by all the 6 SWCNTs at the two highest concentrations, i.e. 8 and 32 mg/L for unmodified and functionalized SWCNTs and 2 and 8 mg/L for metallic and semiconducting SWCNTs, was measured according to

the protocol of Abcam (http://www.abcam.com) and literature [82, 83], using probe 2',7'-Dichlorofluorescin diacetate (DCFDA, Sigma-Aldrich, D6883-50MG). Briefly, GFP-negative yeast strain was incubated in YPD medium overnight, and then seeded in SD medium for 4-6 h at 30 °C. DCFDA probe was then added to reach a final concentration of 25 μM, and incubated for 45 min at 30 °C in dark. The cells were collected, washed once by PBS and then suspended in SD medium. The suspended cells were seeded into clear bottom black side 96-well plate to reach OD600 about 0.3 to 0.4, and chemicals were added to reach the desired final concentration for 2 h exposure. The fluorescence signals were read for 485-nm excitation and 535-nm emission, and the fold change in ROS production was calculated using the following equation: $(F_{test}–F_{test\ blank})/(F_{control}–F_{blank})$, where F_{test}, $F_{test\ blank}$, $F_{control}$, and F_{blank}, represent the fluorescence readings from SWCNT-treated wells, chemical control with probe (no cells), stained control wells, and blank media control with probe (no cells), respectively. The plate reader has been calibrated and verified to provide a linear response for the tested conditions in the assay [84]. The equivalent to H_2O_2 (positive control) was also obtained. The test was conducted in triplicate.

2.5 DNA Damage Alkaline Comet Assay in Human A549 Cells

Alkaline comet assay in human lung epithelial cells A549 (American Type Culture Collection ATCC, Manassas, VA) in response to each SWCNT exposure at 1 mg/mL based on their IC5 concentrations in human A549 (SI Figure S1) or 1% FBS-F12 medium only (as untreated control) for 24 h was performed following the ITRC protocol [85] with the CometAssay 96 Kit (Trevigen Inc., Gaithersburg, MD). Cytotoxicity of plain and functionalized SWCNTs in human A549 cells for 24 h exposure was performed by

first seeding 2×10^4/well of cells in a 96-well plate in the complete growth medium-F12K medium with 10% FBS. Cells are incubated for 24 hours at 37 °C in the presence of 5% CO_2 to reach continuous mono-layer growing. Then the cells were washed by PBS and tested SWCNT samples previously prepared in 1% FBS were added (200 μL/well) in designated wells in triplicates; meanwhile, 200 μL of medium with 1% FBS were added into designated wells in triplicates as untreated controls for each tested sample. The 96-well plate was incubated for 24 hours at 37 °C in the presence of 5% CO_2. The cells were then stained, washed and extracted, and the cell amount was quantified via microplate reader as OD_{630}. Survival ratio was calculated as $OD_{630,\ test}/OD_{630,\ untreated}$. The acute toxicity endpoints were reported as IC5 based on dose-response curves.

All the testing procedures in comet assay were conducted in dark in triplicate. For each treatment, 25 cells were randomly selected and examined using the CASP software (University of Wroclaw, Institute of Theoretical Physics) and the damages were calculated as % Tail DNA. For a given tested SWCNT, it was recognized as genotoxicity positive if the % Tail DNA of treated sample significantly ($p < 0.05$) increased compared to the untreated control.

2.6 Data Analysis

Hierarchical clustering (HCL) was carried out to cluster the 6 SWCNTs across the 6 concentrations according to altered protein expression levels of 74 biomarkers in response to each sample during the 2 h exposure employing the MultiExperiment Viewer (MeV) v4.8 software suite [86]. The relationship among the 36 samples was revealed by the order of complete average linkage clustering according to correlation distance.

To simplify the complex data sets of categories, principal component analysis (PCA) was conducted through examining the components with the highest variance according to their altered protein expression profiles using MultiExperiment Viewer (MeV) v4.8 software suite [86] with centering mode as mean and number of neighbors for KNN imputation as 10.

Furthermore, we performed gene set enrichment analysis (GSEA) to assess the activities of a particular pathway or assembly of proteins by ranking a list of proteins per their PELI values based on the study by Subramanian et al [87]. The significance of each pathway was generated through comparisons between their ranking scores and the associated empirical distributions. The null distributions were obtained via the random permutation of the specific pathway and all others 1000 times.

Additionally, gene ontology (GO) enrichment analysis for determining the significantly represented (overrepresented) biological categories was performed with the Network Ontology Analysis (NOA) method [88] using the selected stress library as the reference set [56]. The activated ORFs that had a mean $PELI_{ORF} > 1.5$ were employed as test sets [56, 76, 89]. A p-value < 0.05 was considered to be statistically significant. GO analysis was performed for the concentrations at which the largest number of proteins (ORFs) were activated, i.e. 32 mg/L for unmodified and functionalized SWCNTs, and 8 mg/L for metallic and semiconducting SWCNTs.

3. Results

3.1 Characterization of SWCNTs

The physical and chemical characteristics of the six SWCNT samples are provided in Table 1. Representative scan electron microscope (SEM) and transmission electron microscope (TEM) images of the samples are shown in Figure 1. Visual inspection indicated that the tubes were highly bundled, with the diameter of bundles as high as 50 nm (versus ~1.2 nm for single tube). We selected three pairs of SWCNTs with different lengths (unmodified short and long), functional groups (short hydroxylated and carboxylated) and electronic structures (short unmodified semiconducting and metallic). The unmodified and functionalized SWCNTs are mixture of approximately 2/3 semiconducting and 1/3 metallic SWCNTs.

All of the carbon nanotubes utilized in this study were pretreated with calcination to remove any amorphouse carbon and hot acid solution wash (concentrated HCl or dilute HNO3) to dissolve any residual surficial metals (Supplementary Information). Therefore, the potential impact of residual metals on the bioassay are likely minimal.

The characterization of aqueous-based SWCNT was performed in SD bioassay medium after 2 h duration, similar to the conditions for the toxicogenomics bioassay, thus the results will be strongly affected by the medium as compared to aqueous SWCNT. The metallic and semiconducting SWCNTs with the lowest zeta potential will be most inclined to aggregate while the functionalized SWCNTs with the highest zeta potential will be the most resistant to aggregation. However, overall the zeta-potentials are quite similar which is likely due to SWCNT interactions with the SD medium. SWCNT Z-average size using DLS is subject to even more error since the light scattering device assumes dense spherical particles and the aggregation of 1D nanotubes will result in low

density non-spherical particles. On top of this, the DLS laser scattering wavelength is 632 nm falls within the metallic SWCNT UV-vis absorption peak.

The measured conductivity for all of the SWCNT samples was quite similar since the measurements were made on vacuum filtered films and thus are a bulk conductivity and not a single particle measurement. Although the conductivity of metallic and semiconducting SWCNTs is significantly different on a single nanotube measurement [90], the bulk measurement could miss the difference since the conductivity will be resisted by the large number of hops an electron must make between tubes over the whole bulk.

Table 1. Characterization of SWCNT. Zeta potential, conductivity, and changes in aggregation size were measured in SD medium during 2 h period, similar to the conditions for bioassays. Mean ± SD. The length range has been supplemented by addition of the mean in parentheses.

SWCNTs		**Long**	**Short**	**-COOH**	**-OH**	**Metallic**	**Semiconducting**
Diameter (nm)		1.2 ± 0.4	1.2 ± 0.4	1.2 ± 0.4	1.2 ± 0.4	1.4 ± 0.3	1.4 ± 0.3
Length (μm)		5-30 (15.0)	0.5-2 (1.0)	0.5-2 (1.0)	0.5-2 (1.0)	0.1-4.0 (1.0)	0.1-4.0 (1.0)
Oxygen content (%)		2.98 ± 0.27	2.43 ± 0.28	6.40 ± 0.67	4.72 ± 0.06	N/A	N/A
Zeta (mV)		-4.16 ± 0.48	-4.77 ± 0.07	-6.01 ± 0.29	-5.23 ± 0.06	-3.15 ± 0.16	-3.25 ± 0.12
Conductivity (mS/cm)		11.20 ± 0.45	10.73 ± 0.42	10.02 ± 0.27	9.24 ± 0.28	11.17 ± 0.69	11.13 ± 0.54
Aggregation size, Z-average (nm)	0h	588.2	379.1	516.9	200.3	429.5	63.88
	2h	755.3	959.2	686.4	719.9	488.1	99.22

Note: N/A: data not available.

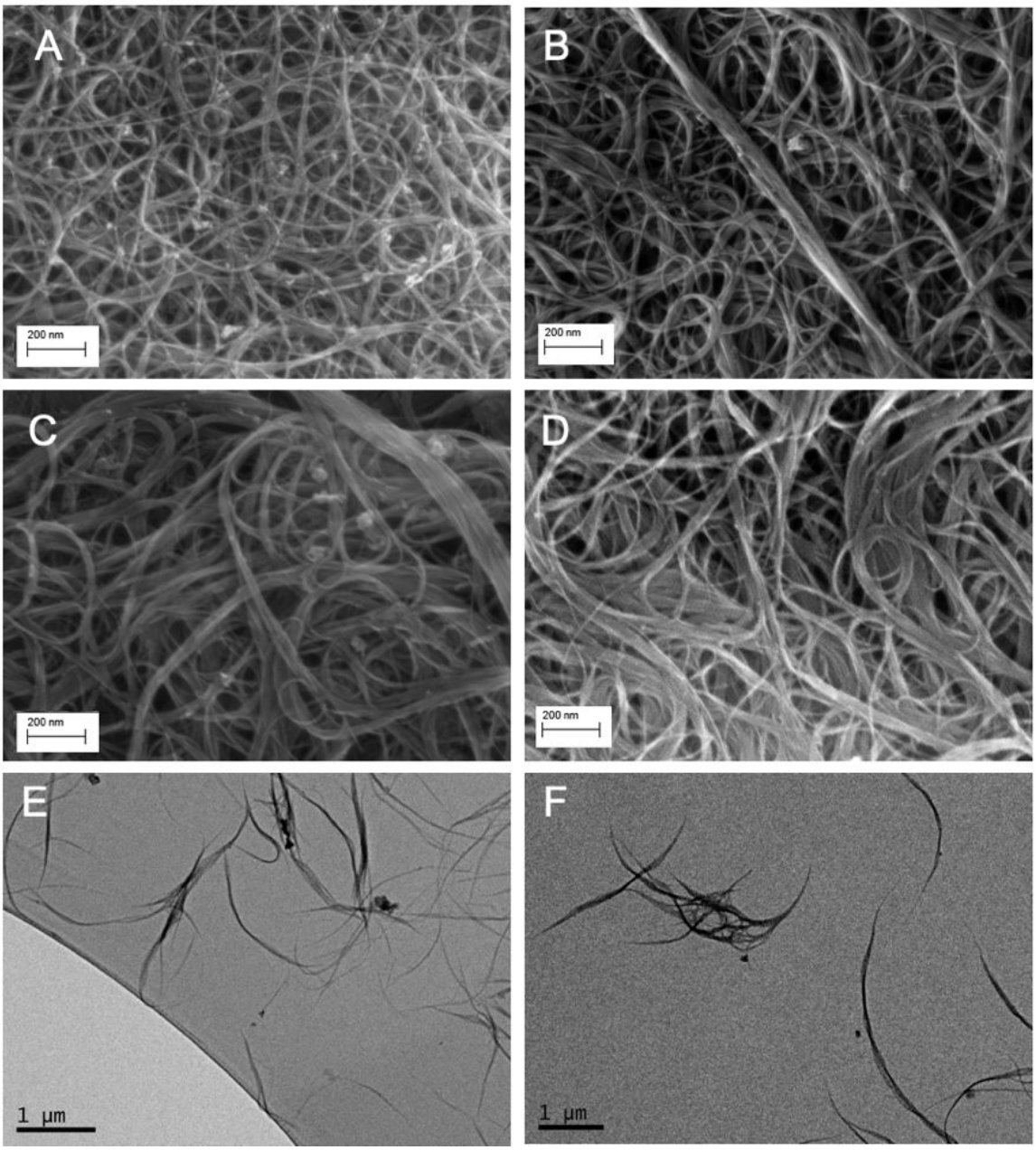

Figure 1. SWCNTs morphology measured using scanning electron microscope (SEM; A - D) and transmission electron microscope (TEM; E - F): (A) long SWCNT, (B) short SWCNT, (C) carboxylated SWCNT, (D) hydroxylated SWCNT, (E) metallic SWCNT, (F) semiconducting SWCNT. The scale is shown at the left bottom corner.

3.2 Distinctive Toxicity Profiles Among Various SWCNTs Revealed by the Quantitative Toxicogenomics Analysis

The high-resolution toxicogenomics assay revealed the distinctive molecular stress response related toxicity profiles among the six SWCNTs with varying characteristics (Figure 2A). The molecular toxicity of SWCNTs is concentration- and structure-dependent, indicating that the varying modification and treatment of the SWCNTs indeed impacted the toxicity fingerprints as results of the changes in surface functionalization, lengths and electronic properties. The magnitude in the induction of protein expression increased with the increase in concentrations for all SWCNTs. In general, the six SWCNTs were separated by clusters, and SWCNTs with the same physicochemical trait (e.g. length) but varying concentrations clustered together, suggesting a more physicochemical-property-dependent toxicity fingerprints. The exception is that at the highest concentrations the different SWCNTs all clustered together. This may be explained by the strong cellular response across all stress pathways and categories exerted by SWCNTs at the highest sub-cytotoxic concentration, which masked the individual CNT-specific stress responses.

The clustered altered protein expression patterns revealed the protein markers and indicated biological processes that shared similar regulation behavior in response to the 6 SWCNTs. There are sub-clusters (i.e. a, b, c) with biomarkers belong to the same stress response categories such as DNA damage and oxidative stress due to their shared co-regulation (Figure 2A). For example, cluster “a” included mostly oxidative stress, DNA damage, and protein damage related biomarkers such as CCS1, YBP1, OGG1, CHK1, UTH1, and OXA1. This cluster of biomarkers exhibited the highest altered protein expression level in response to 4 of the 6 SWCNTs (i.e. unmodified and functionalized SWCNTs) at their highest concentrations, indicating strong DNA and protein damage,

and oxidative effect of these SWCNTs at higher concentrations near the yet sub-cytotoxicity thresholds.

Principal component analysis was performed based on differential protein expression profiles of biomarkers indicative of various cellular stress responses of the 6 SWCNTs with varying structure characteristics (Figure 2B). The results showed that the first two principle components (PCs) explained around 60% of the total variance among all the 6 SWCNTs across 6 concentrations. It is revealed that the studied SWCNTs with different physicochemical properties, and at varying concentrations, were separated with different projection directions, suggesting that they all have distinct toxicity profiles and underlying molecular mechanisms. The lower concentration (≤ 2 mg/L) samples were projected along the left X-axis PC1 direction, while the high concentration (≥ 8 mg/L) samples were scattered towards the right along X-axis, suggesting that the difference in toxicity profiles among varying concentrations was likely captured by the first PC. Along the Y-axis PC2 direction, the metallic SWCNTs were noticeably projected along the upper PC2 direction, indicating a distinct cellular effect likely related to the metallic conductivity. Interestingly, the short and long SWCNTs were projected oppositely along Y-axis, implying their differential molecular toxicity characteristics associated with the length effects. Semiconducting SWCNTs at varying concentrations were all clustered together, close to the lowest concentrations of other SWCNTs, with the lowest magnitude of overall toxicity response.

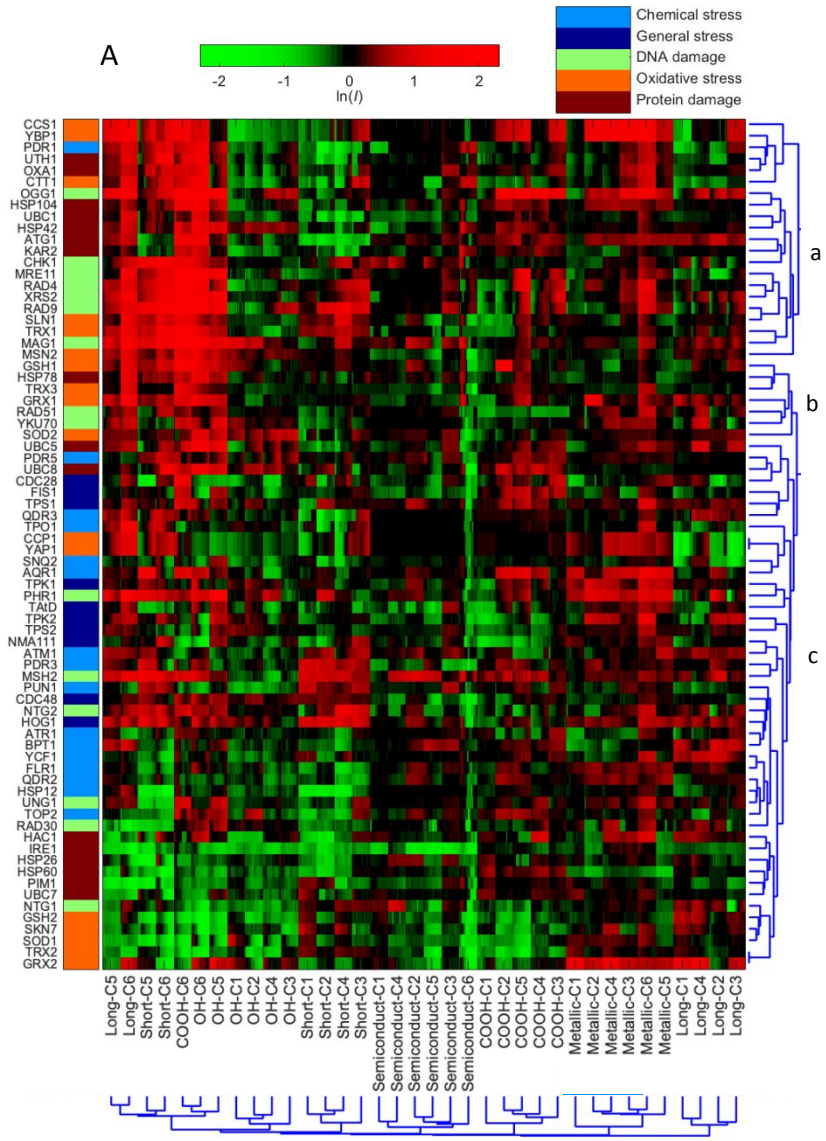
A
-2
-1
0
1
2
ln(I)
Chemical stress
General stress
DNA damage
Oxidative stress
Protein damage
a
b
c
Long-C5
Long-C6
Short-C5
Short-C6
COOH-C6
OH-C6
OH-C5
OH-C1
OH-C2
OH-C4
OH-C3
Short-C1
Short-C2
Short-C4
Short-C3
Semiconduct-C1
Semiconduct-C4
Semiconduct-C2
Semiconduct-C5
Semiconduct-C3
Semiconduct-C6
COOH-C1
COOH-C2
COOH-C5
COOH-C4
COOH-C3
Metallic-C1
Metallic-C2
Metallic-C4
Metallic-C3
Metallic-C6
Metallic-C5
Long-C1
Long-C4
Long-C2
Long-C3

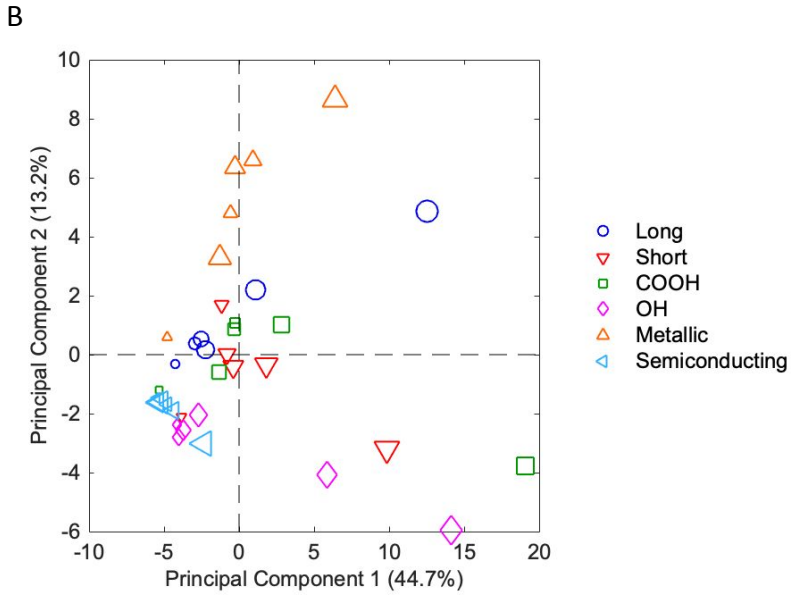
B
Principal Component 2 (13.2%)
Principal Component 1 (44.7%)
Long
Short
COOH
OH
Metallic
Semiconducting

Figure 2. (A) Hierarchical Cluster (HCL) analysis diagram on the basis of differential protein expressions (ln*I*, average of triplicates) of the 74 stress biomarkers in yeast in response to the 6 studied single-walled carbon nanotubes (SWCNTs). The mean natural log of positive induction factors (ln*I*) indicate the magnitude of regulated protein expressions (scaled by the green-black-red color spectrum at the top. Green color spectrum indicates downregulation, and red color spectrum indicates upregulation. The ln*I* values beyond ± 2 were indicated as ± 2). X-axis bottom: sample names and concentrations of the SWCNTs, and cluster root of the samples. C1-C6 indicate concentrations 1-6, which are 0.031, 0.125, 0.5, 2, 8 and 32 mg/L, respectively, for unmodified and functionalized SWCNTs, and 0.0078, 0.031, 0.125, 0.5, 2 and 8 mg/L for metallic and semiconducting SWCNTs. Y-axis left: list of proteins categorized within five stress categories (captions shown at top). Y-axis right: cluster root of stress proteins and sub-clusters a, b, c. All tests were performed in triplicate (n = 3). (B) Principal component analysis (PCA) with differential protein expressions (ln*I*, average of triplicates) in GFP-fused yeast library exposed to the 6 SWCNTs across 6 concentrations. Samples are color-coded and each legend shape indicates one treatment with larger legend size representing the higher concentration.

3.3 Insights into Distinct Molecular Toxicity Mechanisms Revealed by Comparison Among Various SWCNTs

The quantitative toxicity indicators, as PELI values, of the 6 SWCNTs (Figure 3) showed that as the concentration increased, the toxicity levels were generally elevated. Genotoxicity and oxidative stress were the two main stress categories induced upon response to unmodified and functionalized SWCNTs at higher concentrations (8 and 32 mg/L), for which almost all the known DNA damage pathways were induced. The dominant molecular response seemed to be DNA stress for all samples disregarding the functionalization and length, which was also confirmed by GSEA analysis (Figure 3 and SI Table S2; detailed results and discussion described below). This is consistent with the previous finding indicating that single-stranded DNA possessed the ability to wrap CNT [91]. Additionally, functionalization of SWCNTs led to elevated overall toxicity, especially notably greater genotoxicity than unmodified SWCNTs at the higher concentration range. Semiconducting SWCNT exhibited the lowest and nearly marginal observable toxicity (PELI < 1.5) among all SWCNTs.

The PELI-based molecular endpoint PELI1.5 (mg/L) was determined from the 4PL nonlinear concentration-response curves (SI Figure S3) at the studied concentration range, as shown in Table 2. PELI1.5 marks the beginning of observable toxicological effects (PELI = 1.5), and can quantitatively reflect toxicity levels at the lower concentration range. Consistent with toxicity level profiles and GSEA analysis, the PELI1.5 of DNA damage was the lowest among the five stress categories for each SWCNT, meaning that DNA damage category exhibited the highest toxicity level among all categories. Short SWCNT showed notably lower PELI1.5 in general, DNA, oxidative,

protein, and overall stress than long SWCNT, indicating a higher toxicity for short SWCNT. Although the PELI1.5 of oxidative stress was comparable for the two functionalized SWCNTs, carboxylated SWCNT had lower PELI1.5 in chemical stress, DNA damage, protein damage and total stress than the hydroxylated tube variant, indicating that carboxylation induced a higher SWCNT toxicity compared to hydroxylation. Metallic SWCNT exhibited a greater DNA damage capability than semiconducting variant based on PELI1.5, which is consistent with toxicity level and protein expression profiles.

Furthermore, toxic equivalents geno-TEQ1.5 and oxi-TEQ1.5 induced by each SWCNT at PELI1.5 were calculated using MMC and H_2O_2 as the reference compound, respectively, as listed in Table 2. It is worth noting that the PELI1.5 was determined at the tested concentration range (0.031-32 mg/L for unmodified and functionalized SWCNTs), and from the concentration-response curves, short SWCNT has a $PELI1.5_{geno}$ less than 0.031 mg/L, and thus has the highest genotoxic equivalent. In contrast, based on PELI1.5 of oxidative stress, metallic SWCNT possessed the highest oxidative stress equivalent in reference to H_2O_2.

The stress categories were analyzed by GSEA to further compare toxicity responses and potential MOAs among all the 6 SWCNTs (SI Table S2). Results indicated that DNA damage and oxidative stress were the main MOA for all samples disregarding the functionalization and length. In particular, DNA damage was the dominant stress category. Oxidative stress was significantly enriched for long and semiconducting SWCNTs at the highest concentrations, and for hydroxylated and metallic SWCNTs at the lower concentrations.

GO enrichment analysis was performed for the activated ORFs ($PELI_{ORF} > 1.5$) in yeast cells in response to the 6 SWCNTs exposure at their highest concentrations, i.e. 32 mg/L for unmodified and functionalized SWCNTs, and 8 mg/L for metallic and semiconducting SWCNTs, which had the largest number of ORFs activated. The overrepresented (*p*-value < 0.05) GO biological categories, i.e. biological processes, cellular components and molecular functions, are listed in Table S3. Results showed that the biological processes induced by the 32 mg/L long SWCNT were mainly associated with cellular response to stimulus and stress, and response to DNA damage stimulus, indicating DNA stress was one of the main stress categories, which was consistent with GSEA results. Additionally, the significantly represented GO cellular components suggesting the macromolecules such as protein and DNA might be the main targets for long-SWCNT-induced toxicity. For the 32 mg/L short SWCNT, macromolecule modification, post-translational protein modification, and phosphorylation were mainly induced. Moreover, transferase activity, specifically transferring phosphorus-containing groups such as diphosphate or nucleotides was induced by short SWCNT.

Regarding the two functionalized SWCNTs, negative regulation of biological process and cellular process were mainly induced by the carboxylated SWCNT, implying that yeast cells might undertake down-regulation of some biological and cellular processes to stop or reduce their rate or extent in response to carboxylated SWCNT exposure. Additionally, macromolecular complex and nuclear part might be the main target sites by carboxylated SWCNT, indicated by the overrepresented GO cellular components. While for the 32 mg/L hydroxylated SWCNT, response to stimulus, negative regulation of biological and cellular process, and autophagy were induced.

DNA-damage-related biological processes, such as DNA metabolic process, response to DNA damage stimulus, and DNA repair were significantly induced by the 8 mg/L metallic SWCNT, and nucleus might be the main target site indicated by the overrepresented GO cellular components. Regarding the semiconducting SWCNT, biological processes such as response to stimulus and oxidative stress, and cell redox homeostasis, and molecular functions oxidoreductase activity were overrepresented, indicating oxidative stress is the main toxicity category, which is consistent with GSEA analysis (Figure 3 and SI Table S2).

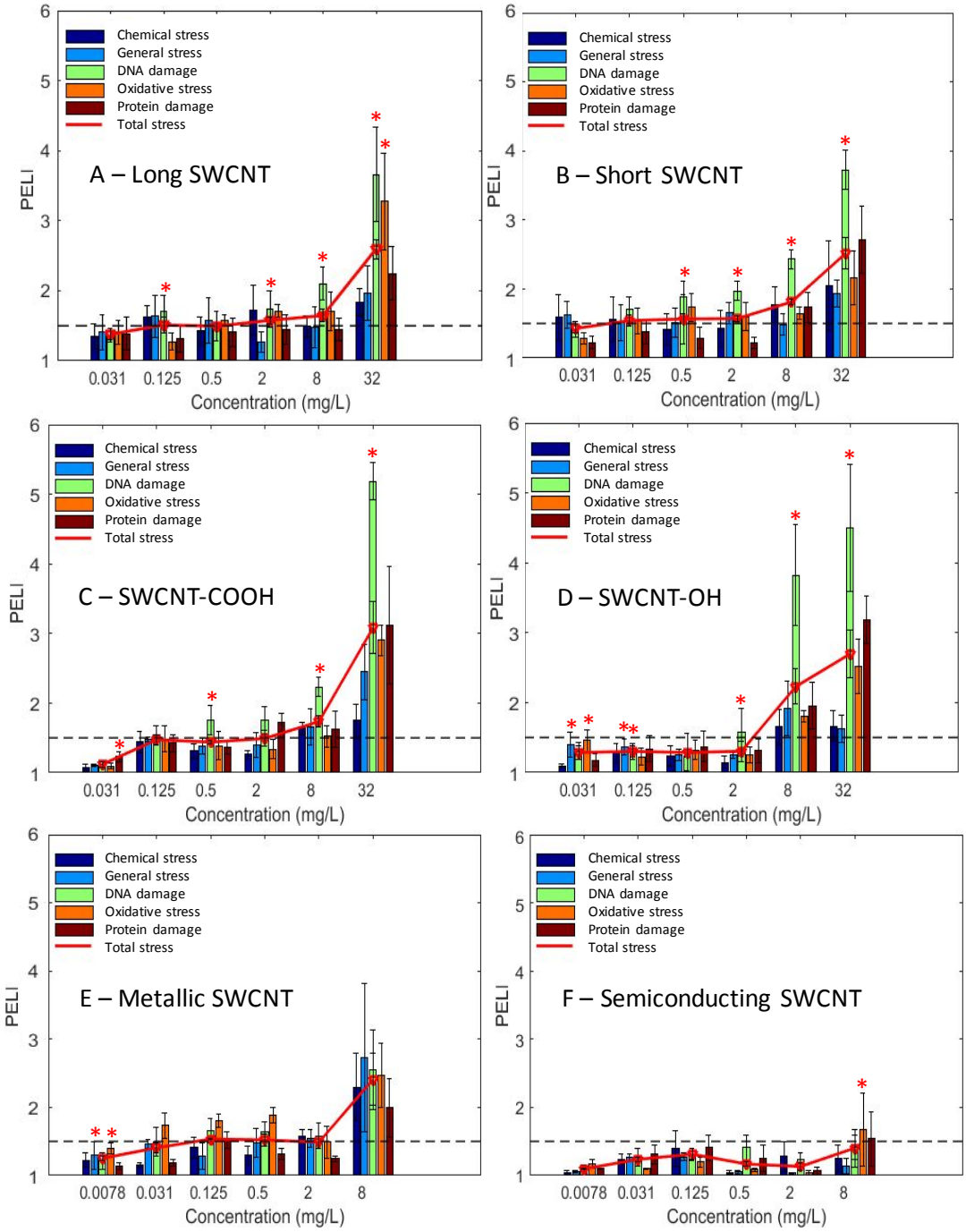

Figure 3. Quantitative molecular toxicity profiles of the 6 studied single-walled carbon nanotubes (SWCNTs) in terms of the PELI values for the 5 stress categories and total PELI: (A) long SWCNT, (B) short SWCNT, (C) carboxylated SWCNT, (D) hydroxylated SWCNT, (E) metallic SWCNT, (F) semiconducting SWCNT. X-axis: concentrations of examined SWCNTs (mg/L). Y-axis: PELI as molecular toxicity endpoint. Mean ± SD; replication number n = 3. The "*" indicates the enriched stress categories revealed by GSEA.

Table 2. Summary of PELI-based molecular endpoint PELI1.5 (mg/L) and toxic equivalents geno-TEQ1.5 and oxi-TEQ1.5. PELI1.5 was determined from the Four Parameter Logistic (4PL) nonlinear concentration-response curves (SI Figure S3) at the studied concentration range for the 5 stress and total categories. Toxic equivalents geno-TEQ1.5 and oxi-TEQ1.5 are for genotoxicity and oxidative stress, respectively, induced by each SWCNT at PELI1.5, using mitomycin C (MMC) and H_2O_2 as the reference compound, respectively.

SWCNTs	PELI1.5 (mg/L)						TEQ1.5	
	Chemical	General	DNA	Oxidative	Protein	Total	Geno-	Oxi-
Long	0.30	8.36	0.048	1.52	10.23	1.58	14.98	2.24
Short	5.22	< 0.031	< 0.031	0.24	7.39	0.14	> 23.19	14.18
-COOH	4.99	3.85	0.209	7.29	2.801	2.98	3.44	0.467
-OH	6.58	2.91	1.52	7.47	4.88	3.89	0.47	0.456
Metallic	1.46	1.51	0.48	< 0.0078	N/A	1.93	1.50	> 436.3
Semiconducting	N/A	N/A	N/A	7.57	7.86	N/A	N/A	0.45

Note: N/A: data not available. PELI1.5 is not available when the concentration-response curve falls below the line PELI = 1.5 at the highest studied concentration.

3.4 Conventional Phenotypic Toxicity Endpoints of SWCNTs and Comparison with Molecular Toxicity Endpoints comparisons

To validate and compare molecular endpoints with phenotypic endpoints, we also performed oxidative stress related ROS production measurement in yeast cells and genotoxicity alkaline comet assay in human A549 cells for the 6 SWCNTs. The correlation between molecular and phenotypic endpoints can evaluate and quantify the

capability of the quantitative molecular disturbance quantifier based on altered expression of key proteins involved in oxidative stress and DNA damage pathways to capture the ROS production and DNA damage potential, and therefore to predict phenotypical outcomes in terms of ROS production and DNA damage phenotypic endpoints, which are shown in Figure 4.

The ROS production comparison among all SWCNTs are shown in Figure 4A. Results showed that the ROS production induced in yeast cells increased as the concentrations increased for each SWCNT. Additionally, the long and hydroxylated SWCNTs induced the highest ROS production at 8 and 32 mg/L. Furthermore, we examined the consistency and correlation between ROS production and toxicogenomics assay endpoints PELI values induced by each SWCNT at the same concentration. The PELI values of oxidative stress and total stress had a good correlation with ROS production (r = 0.8642 and 0.9501, respectively) (Figure 5).

The DNA damage results via comet assay revealed that all SWCNTs except the semiconducting one exhibited the positive genotoxicity in human A549 cells (Figure 4B), which are consistent with the toxicogenomics assay results. Furthermore, the phenotypic genotoxicity endpoints generated from comet assay in human cells were in a good agreement with the molecular endpoints $PELI_{geno}$ (r = 0.9198) (Figure 5). This suggested that the biomarkers ensemble selected in the toxicogenomics assay for DNA damage stress categories were cable to capture and predict the potential DNA-damage, as shown in our previous studies [20,47-49.] Comet assay detects DNA strand breaks resulted from various DNA damages, including single strand breaks, double strand breaks, alkali-labile sites, incomplete excision repair sites, and crosslinks (DNA-DNA or DNA-protein) [92],

therefore cautions should be taken in correlating Comet assay results with individual biomarker or damage pathway [93]. This highlights the advantages of real-time multi-biomarker and multi-pathway ensemble-based approaches. In addition, possible interferences of NMs on Comet assay, as suspected by Lin et al [93], require considerations as well.

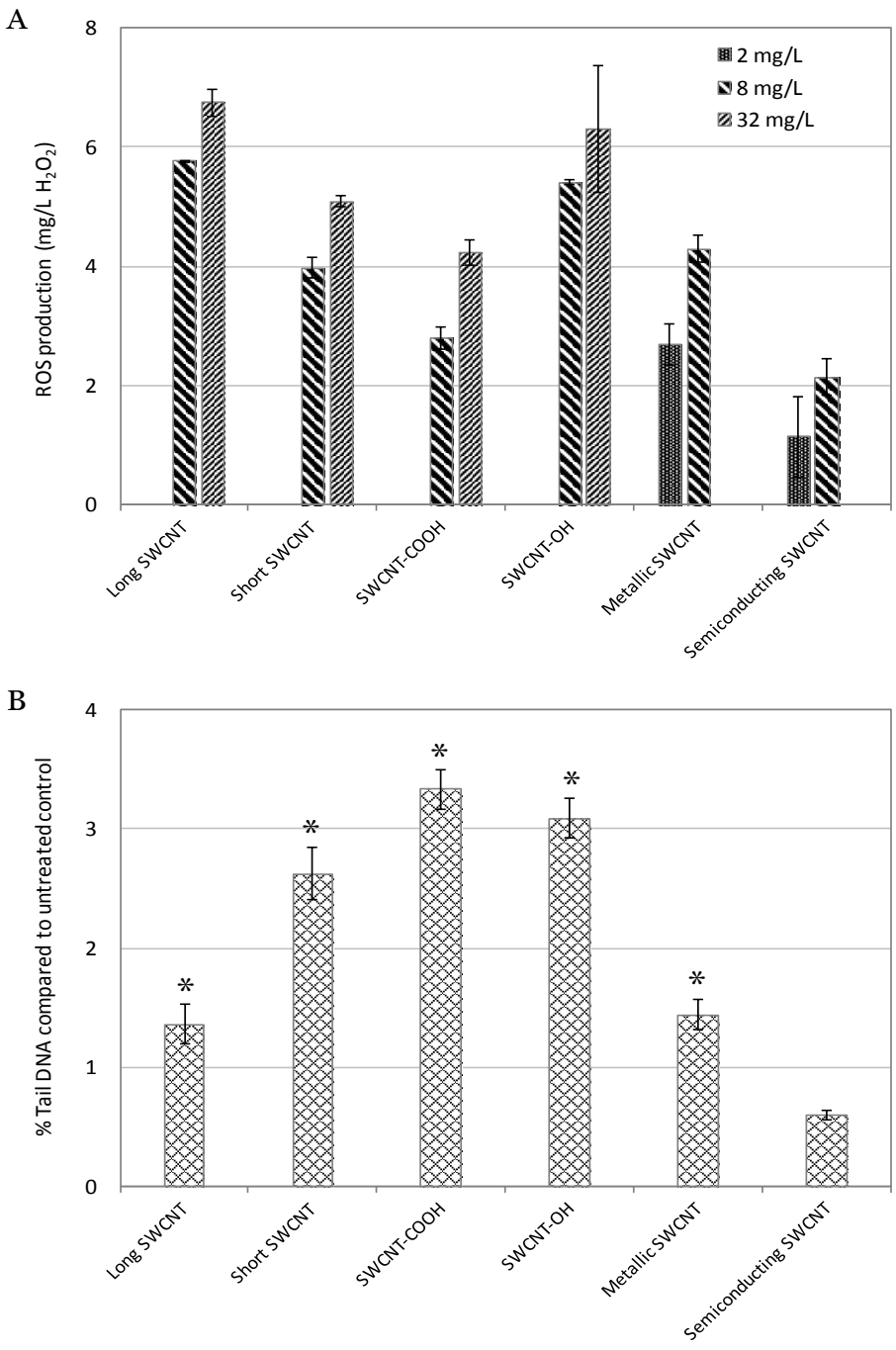

Figure 4. (A) Intracellular ROS production (equivalent to mg/L H_2O_2) in yeast cells induced by the 6 tested single-walled carbon nanotubes (SWCNTs), and (B) % Tail DNA compared to untreated control determined by alkaline comet assay for the 6 SWCNTs. The % Tail DNA compared to untreated control indicates DNA damage caused in human A549 cells by the 6 SWCNTs. (A) and (B): X-axis bottom: name of the 6 SWCNTs; Y-axis: (A) ROS production (equivalent to mg/L H_2O_2), and (B) % Tail DNA compared to untreated control. The "*" indicates significantly higher than untreated control ($p < 0.05$). Mean ± SD. For ROS production, n = 3; for comet assay, n = 4.

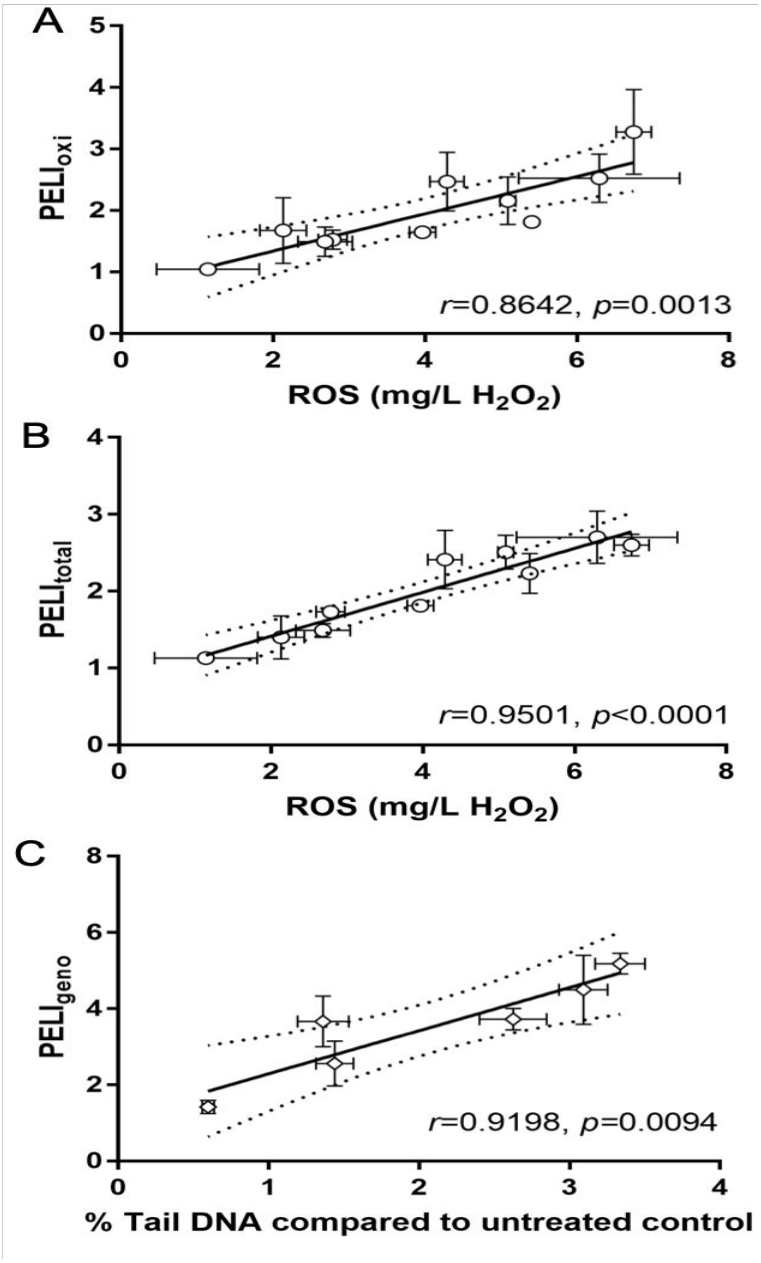

Figure 5. Correlation of intracellular ROS generation (equivalent to mg/L H_2O_2) with $PELI_{oxi}$ (A) and $PELI_{total}$ (B) in yeast, and correlation of % Tail DNA compared to untreated control with $PELI_{geno}$ for the 6 tested single-walled carbon nanotubes (SWCNTs) (C). The % Tail DNA compared to untreated control examined by alkaline comet assay indicates DNA damage caused in human A549 cells by the 6 SWCNTs. The 95% confidence intervals are indicated by the dash lines. (A) and (B): X-axis bottom: ROS production in yeast equivalent to mg/L H_2O_2; Y-axis: $PELI_{oxi}$ (A) or $PELI_{total}$ (B) in yeast assay. (C) X-axis bottom: % Tail DNA compared to untreated control; Y-axis: $PELI_{geno}$ in yeast assay. *r* indicates Pearson correlation coefficient; *p* value shows whether the correlation is significantly linear. Mean ± SD. For ROS production, n = 3; for comet assay, n = 4. An error bar was not shown when it was smaller than marker size.

4. Discussion

The ROS generated from the interaction between engineered CNMs (including SWCNTs) with biological molecules, which thus lead to oxidative stress, have been proposed as possible mechanisms involved in their nanotoxicity [94, 95]. ROS are well known to have both harmful and beneficial effects on biological systems. The deleterious influence on cells has been demonstrated to generally result in DNA damage, oxidation of amino acids in proteins and fatty acids in lipids (lipid peroxidation), as well as oxidative inactivation of specific enzymes via co-factor oxidation [96]. Our results from molecular toxicogenomics assay and conventional phenotypic assay indicated that all the 6 studied SWCNTs can induce oxidative stress and ROS production in yeast cells in a concentration-dependent pattern.

Genotoxicity is the main toxicity category for unmodified and functionalized SWCNTs in our study. Concerns have been raised about the genotoxic effects of nanomaterials in recent years [97], which should be carefully investigated, considering that the instability of genetic materials is directly related to the cancer development [98]. Genotoxicity caused by nanomaterials could be ascribed to several reasons, such as direct interaction of the particles with DNA or other cellular components, indirect damage induced by ROS, as well as release of toxic ions [99]. The quantitative toxicogenomics-based genotoxicity indicator PELI values were higher than those for the oxidative stress effects, suggesting that, the mechanical injury, rather than, or in addition to oxidative effects, was likely responsible for the DNA damage induced by SWCNTs [100]. Specifically, SWCNTs possibly penetrated cell nucleus via nucleopores, followed by degrading the double helix structure of DNA [101].

In spite of the similarity in the oxidative stress and genotoxicity commonly exerted by all the 6 SWCNTs, our results further revealed more detailed molecular toxicity natures and fingerprints that were differentially affected by their physicochemical properties, i.e. lengths, surface functional groups and electronic structure as discussed below.

4.1 Effect of Lengths on Toxicity of SWCNTs

Comparison of quantitative toxicogenomics assay endpoints PELI values suggested that the short SWCNT (0.5-2 μm) had a higher toxicity level than long SWCNT (5-30 μm) (Table 2). Additionally, both the stress response profiling and PCA results revealed distinguishable molecular toxicity fingerprints for the two SWCNTs with different lengths (Figure 2).

The documented data citing *in vitro* toxicity of SWCNTs with different lengths are inconsistent. The interactions between SWCNTs and cells include internalization and penetration [102-104]. Phagocytosis was regarded as the most critical pathway for internalization of SWCNTs having 1 μm or longer length and thus for SWCNT related toxicity [102, 105]. Therefore, cells that cannot uptake nanoparticles via phagocytosis should have higher vulnerability to CNTs with consequently lower toxicity [106]. In contrast, Cui et al. investigated the uptake and exocytosis of SWCNTs in three lengths in macrophages, and found that the cellular accumulation of SWCNTs was independent on length [107]. In this study, the size of yeast cells (3-4 μm) is comparative to that of CNTs, which makes the phagocytosis of nanotubes by yeast cells not likely, therefore the expected difference in toxicity effects resulted from preference in phagocytosis due to SWCNT length may not be as evidence.

The other mode of action of SWCNTs to cells is penetration [103], which is likely the main interaction mode between yeast cells and the studied SWCNTs considering their comparative sizes. Rotoli et al. compared the effects of two SWCNTs with length of 0.5-100 μm and 0.5-2 μm on human lung cancer cell line Calu-3, and the results indicated that only shorter SWCNTs induce a significant decrease in cell viability [108]. Our results showed that the varying CNT lengths not only resulted in significant difference in the toxicity endpoints magnitude between the SWCNTs based on PELI values, but also induced the differences in their observably distinguishable molecular impacts on cells elucidated by the high-resolution molecular response profiles, which may entail certain different toxicological outcomes. Specifically, the SWCNT with a shorter length showed a higher toxicity, which might be due to that the short tubes are more mobile and less prone to aggregation, making the penetration easier compared to long tubes. In addition, a number of key biomarkers showed up-regulated expression in response to short SWCNT only and not to long SWCNT, such as cell wall integrity related plasma membrane protein PUN1, apoptosis related protein NMA111, and cytosolic unfolded protein response (cytUPR) related protein UBC8 (SI Figure S2).

4.2 Effect of Functional Groups on Toxicity of SWCNTs

The results in our study showed that DNA damage and genotoxicity was the dominant toxicity category for both carboxylated and hydroxylated SWCNTs (Figure 3). Based on quantitative toxicogenomics assay endpoints, carboxylated SWCNT induced a greater genotoxicity, chemical stress, protein damage and overall toxicity compared to hydroxylated one, while the oxidative stress level was comparable for both. This might be partially explained by that carboxylated SWCNT has a higher permanent negative

charge and is significantly more water stable. Functionalization has been increasingly employed to modify the hydrophobicity or hydrophilicity of nanoparticles [109], facilitating covalent biomolecule binding [110] and providing active sites to immobilize target enzymes [111]. SWCNT functionalization modifies their surface chemistry and dispersion, and thus may influence their toxicological effects. Yang et al. found a higher toxicity of functionalized SWCNTs and attributed this to their higher solubility and dispersion in water [112], and thus they had a higher chance to bind with the protein, peptide or oligonucleotide [96].

A study conducted by Mrakovcic et al. showed carboxylated short SWCNTs (1-2 μm) exhibited higher genotoxicity in V79 Chinese hamster fibroblasts and human A549 cells than unmodified SWCNTs [30]. Others also showed evidence that COOH modified SWCNTs exhibited higher toxicity than unmodified SWCNTs in human endothelial cells (HUVEC) [113], as well as in fish embryos [114]. Our finding confirmed the elevated toxicity related to functionalization on SWCNT at the higher concentration range, as discussed above. Furthermore, the finer-resolution differences between the two different functional groups, namely COOH versus OH, in their cellular molecular toxicity responses were revealed for the first time. For example, signal transduction related biomarker CDC28 was up-regulated in response to carboxylated SWCNT only; while only hydroxylated SWCNT induced the up-regulation of protein RAD30 that is related to translesion synthesis (TLS) DNA repair pathway.

4.3 Effect of Electronic Structure on SWCNT Toxicity

Comparison of the toxicity between metallic and semiconducting SWCNTs showed dramatic differences in their toxicity levels and stress response profiles, with

metallic SWCNT exerting relatively higher toxicity, while semiconducting SWCNT showing the lowest and nearly no observable toxicity (PELI < 1.5) (Figures 2 and 3). Various studies demonstrated semiconducting SWCNTs were significantly less reactive than metallic SWCNTs with similar dimensions [115-119]. The higher electron density and conductivity near the SWCNT Fermi level could be attributed to the higher reaction rate for metallic SWCNTs. Vecitis et al. showed that the metallic SWCNT had a higher cytotoxicity than semiconducting SWCNTs in *E. coli*, and proposed that the metallic SWCNT facilitated cellular oxidation by conductively bridging over the lipid bilayer and then electronically aiding oxidation of some key polypeptides such as glutathione that plays a crucial role in maintaining cell redox environment and its significant oxidation leads to cell death. Another mechanism proposed is that the metallic SWCNTs could induce direct oxidization of bacteria through a process like Fermi level equilibration [120, 121]. Our results confirmed that metallic SWCNT indeed led to a higher molecular toxicity than semiconducting SWCNT. This might be attributed to that the micrometer length and conductive characteristics of metallic SWCNTs enabled the potential "short-circuit" of cells by acting as conductive bridges over the insulating lipid bilayers, accompanying by release of cellular energy into the external environment.

Moreover, the high-resolution toxicogenomics assay depicted distinctive molecular stress response profiles for metallic and semiconducting SWCNTs, revealing that a large number of key biomarkers were significantly upregulated in response to metallic SWCNT but not to semiconducting (Figure 2 and SI Figure S2). For example, chemical stress related protein SNQ2 that is a ATP-binding cassette (ABC) transporter, general stress related protein FIS1 involved in mitochondrial fission and peroxisome

abundance, oxidative stress regulators SKN7, and DNA repair proteins RAD30 for TLS, RAD4 for nucleotide excision repair (NER), and PHR1 for direct reversal repair (DRR) exhibited significant upregulation only with metallic SWCNT. It is recognized that there is still considerable pathway level detail that is yet to be elucidated and the differences between yeast and higher organisms are bound to exist. Therefore, the method described here is more suitable for Tox21 vision tiered testing as screening, prioritization and initial assessment of toxicity, especially for environmental applications that have challenges in high resource cost-demand due to large number of samples/conditions. This will help guide and prioritizing the resources for further evaluation in specific and relevant biological systems.

5. Conclusions

This study quantitatively compared the cellular toxicity profiles and mechanisms among 6 SWCNTs with varying lengths, functional groups and electronic structures with the object to elucidate the toxicological effects of SWCNTs and their dependence on physicochemical properties. The results revealed that DNA damage and oxidative stress seemed to be the dominant molecular effects for all SWCNTs, although the molecular toxicity profiles were distinct indicating distinguishable and SWCNT property-dependent toxicity effects and mechanisms among the SWCNTs with varying lengths, functionalization and electronic structures. Comparison of quantitative toxicogenomics assay endpoints PELI values suggested that the short SWCNT (0.5-2 μm) had a higher toxicity level than long SWCNT (5-30 μm) and they have distinguishable molecular toxicity fingerprints with short SWCNT having the highest oxidative stress effects in

contrast to more pronounced DNA damage effects by long SWCNT. Due to the comparable size of yeast cells (3-4 μm) to that of CNTs, the phagocytosis of nanotubes by yeast cells is not likely and penetration is likely the main interaction mode between yeast cells and the studied SWCNTs. Functionalization also impacts the toxicity nature. Carboxylated SWCNT induced a greater genotoxicity, chemical stress, protein damage and overall toxicity compared to hydroxylated one, while the oxidative stress level was comparable for both. This might be partially explained that carboxylated SWCNT has a higher permanent negative charge with higher water solubility. Comparison of the toxicity between metallic and semiconducting SWCNTs showed dramatic differences in their toxicity levels and stress response profiles, with metallic SWCNT exerting relatively higher toxicity than semiconducting SWCNT that has nearly no observable toxicity. This confirms the previous observation that the metallic SWCNT had a higher cytotoxicity than semiconducting SWCNTs in *E. coli*. The results seem to support the hypothesis that that metallic SWCNTs enabled the potential "short-circuit" of cells by acting as conductive bridges over the insulating lipid bilayers and then electronically aiding oxidation.

The data generated in this study can be used to develop prototype nanotoxicity Quantitative Structure Activity Relationship (QSAR) models with hierarchical structures that integrates current QSAR framework with molecular bioassay information through correlative links among nanomaterial descriptors, nanotoxicity mechanism-specific molecular endpoints and phenotypic nanotoxicity endpoints. The comprehensive comparison of cellular toxicity profiles and mechanisms among the 6 SWCNTs can bridge the knowledge gap on relationship between nanomaterial toxicity mechanisms and

physicochemical properties. The high-resolution molecular stress response profile and toxicity level comparisons would advance and contribute to a systematic understanding of CNT toxicity, and is expected to be a screening tool to guide for nanomaterial manufacturing and risk management. In addition, the knowledge on the impact of single CNT property factor as elucidated in this study would facilitate the assessment of synergy of multiple property variables, which warrants future investigation.

Conflicts of interest

There are no conflicts to declare.

Acknowledgements

The authors acknowledge support from the United States National Science Foundation (NSF, CBET-1437257, IIS-1546428) and National Institute of Environmental Health Sciences (P42ES017198).

References

1. R. J. Chen, S. Bangsaruntip, K. A. Drouvalakis, N. W. S. Kam, M. Shim, Y. M. Li, W. Kim, P. J. Utz and H. J. Dai, Noncovalent functionalization of carbon nanotubes for highly specific electronic biosensors, *Proc. Natl. Acad. Sci. U.S.A.*, 2003, **100**, 4984-4989.
2. M. F. Zhang and M. Yudasaka, Carbon nanohorns and their high potential in biological applications, *Carbon Nanostruct.*, 2016, 77-107.
3. N. Belkhamssa, J. P. da Costa, C. I. L. Justino, P. S. M. Santos, S. Cardoso, A. C. Duarte, T. Rocha-Santos and M. Ksibi, Development of an electrochemical biosensor for alkylphenol detection, *Talanta*, 2016, **158**, 30-34.
4. F. H. Panahi, S. J. Peighambardoust, S. Davaran and R. Salehi, Development and characterization of PLA-mPEG copolymer containing iron nanoparticle-coated

carbon nanotubes for controlled delivery of Docetaxel, *Polymer*, 2017, **117**, 117-131.

5. A. Ortega-Guerrero, J. M. Espinosa-Duran and J. Velasco-Medina, TRPV1 channel as a target for cancer therapy using CNT-based drug delivery systems, *Eur. Biophys. J. Biophy.*, 2016, **45**, 423-433.
6. N. W. S. Kam, M. O'Connell, J. A. Wisdom and H. J. Dai, Carbon nanotubes as multifunctional biological transporters and near-infrared agents for selective cancer cell destruction, *Proc. Natl. Acad. Sci. U.S.A.*, 2005, **102**, 11600-11605.
7. A. M. Diez-Pascual, Tissue engineering bionanocomposites based on poly(propylene fumarate), *Polymers-Basel*, 2017, **9**.
8. A. Gupta, T. A. Liberati, S. J. Verhulst, B. J. Main, M. H. Roberts, A. G. R. Potty, T. K. Pylawka and S. F. El-Amin, Biocompatibility of single-walled carbon nanotube composites for bone regeneration, *Bone Joint Res.*, 2015, **4**, 70-77.
9. P. Galvan-Garcia, E. W. Keefer, F. Yang, M. Zhang, S. Fang, A. A. Zakhidov, R. H. Baughman and M. I. Romero, Robust cell migration and neuronal growth on pristine carbon nanotube sheets and yarns, *J. Biomat. Sci-Polym. E.*, 2007, **18**, 1245-1261.
10. N. Gulati and H. Gupte, Two faces of carbon nanotube: toxicities and pharmaceutical applications, *Crit. Rev. Ther. Drug*, 2012, **29**, 65-88.
11. E. Petersen, D. Flores-Cervantes, T. Bucheli, L. Elliott, J. Fagan, A. Gogos, S. Hanna, R. Kagi, E. Mansfield, A. R. M. Bustos, D. L. Plata, V. Reipa, P. Westerhoff and M. Winchester, Quantification of carbon nanotubes in

environmental matrices: current capabilities, case studies, and future prospects, *Environ. Sci. Technol.*, 2016, **50**, 4587-4605.

12. A. Schierz, B. Espinasse, M. R. Wiesner, J. H. Bisesi, T. Sabo-Attwood and P. L. Ferguson, Fate of single walled carbon nanotubes in wetland ecosystems, *Environ. Sci. Nano*, 2014, **1**, 574-583.
13. N. C. Mueller and B. Nowack, Exposure modeling of engineered nanoparticles in the environment, *Environ. Sci. Technol.*, 2008, **42**, 4447.
14. B. Nowack, R. M. David, H. Fissan, H. Morris, J. A. Shatkin, M. Stintz, R. Zepp and D. Brouwer, Potential release scenarios for carbon nanotubes used in composites, *Environ. Int.*, 2013, **59**, 1-11.
15. F. Gottschalk, T. Sun and B. Nowack, Environmental concentrations of engineered nanomaterials: Review of modeling and analytical studies, *Environ. Int.*, 2013, **181**, 287-300.
16. E. J. Petersen, Q. Huang and W. J. Weber, Bioaccumulation of radio-labeled carbon nanotubes by *Eisenia foetida*, *Environ. Sci. Technol.*, 2008, **42**, 3090-3095.
17. R. Bjorkland, D. Tobias and E. J. Petersen, Increasing evidence indicates low bioaccumulation of carbon nanotubes, *Environ. Sci. Nano*, 2017, **4**, 747-766.
18. S. J. Sarma, I. Bhattacharya, S. K. Brar, R. D. Tyagi and R. Y. Surampalli, Carbon nanotube-bioaccumulation and recent advances in environmental monitoring, *Crit. Rev. Environ. Sci. Technol.*, 2015, **45**, 905-938.
19. C. Larue, M. Pinault, B. Czarny, D. Georgin, D. Jaillard, N. Bendiab, M. Mayne-L'Hermite, F. Taran, V. Dive and M. Carrière, Quantitative evaluation of multi-

walled carbon nanotube uptake in wheat and rapeseed, *J. Hazard. Mater.*, 2012, **227-228**, 155-63.

20. E. J. Petersen, J. Akkanen, J. V. K. Kukkonen and W. J. Weber, Biological uptake and depuration of carbon nano-tubes by *Daphnia magna*, *Environ. Sci. Technol.*, 2009, **43**, 2969-2975.

21. E. J. Petersen, R. A. Pinto, D. J. Mai, P. F. Landrum and W. J. Weber, Influence of polyethyleneimine fraftings of multi-walled carbon nanotubes on their accumulation and elimination by and toxicity to *Daphnia magna*, *Environ. Sci. Technol.*, 2011, **45**, 1133-1138.

22. P. Ravichandran, S. Baluchamy, R. Gopikrishnan, S. Biradar, V. Ramesh, V. Goornavar, R. Thomas, B. L. Wilson, R. Jeffers, J. C. Hall and G. T. Ramesh, Pulmonary biocompatibility assessment of inhaled single-wall and multiwall carbon nanotubes in BALB/c Mice, *J. Biol. Chem.*, 2011, **286**, 29725-29733.

23. L. C. Ong, F. F. L. Chung, Y. F. Tan and C. O. Leong, Toxicity of single-walled carbon nanotubes, *Arch. Toxicol.*, 2016, **90**, 103-118.

24. A. M. Swidwinska-Gajewska and S. Czerczak, Carbon nanotubes - characteristic of the substance, biological effects and occupational exposure levels, *Med. Pr.*, 2017, **68**, 259-276.

25. Y. Qin, S. N. Li, G. Zhao, X. H. Fu, X. P. Xie, Y. Y. Huang, X. J. Cheng, J. B. Wei, H. G. Liu and Z. F. Lai, Long-term intravenous administration of carboxylated single-walled carbon nanotubes induces persistent accumulation in the lungs and pulmonary fibrosis via the nuclear factor-kappa B pathway, *Int. J. Nanomed.*, 2017, **12**, 263-277.

26. J. Yuan, H. Gao, J. Sui, H. Duan, W. N. Chen and C. B. Ching, Cytotoxicity evaluation of oxidized single-walled carbon nanotubes and graphene oxide on human hepatoma HepG2 cells: an iTRAQ-coupled 2D LC-MS/MS proteome analysis, *Toxicol. Sci.*, 2012, **126**, 149-161.

27. L. L. Zhou, H. J. Forman, Y. Ge and J. Lunec, Multi-walled carbon nanotubes: a cytotoxicity study in relation to functionalization, dose and dispersion, *Toxicol. In Vitro*, 2017, **42**, 292-298.

28. C. J. Yoo, Y. J. Kim, U. Lee and Y. M. Yoo, Cytotoxicity of single-walled carbon nanotubes in human neural precursor cells on monolayer culture and rat brain slices, *J. Nanosci. Nanotechno.*, 2016, **16**, 7677-7683.

29. J. S. Kim, K. S. Song and I. J. Yu, Evaluation of in vitro and in vivo genotoxicity of single-walled carbon nanotubes, *Toxicol. Ind. Health*, 2015, **31**, 747-757.

30. M. Mrakovcic, C. Meindl, G. Leitinger, E. Roblegg and E. Frohlich, Carboxylated short single-walled carbon nanotubes but not plain and multi-walled short carbon nanotubes show in vitro genotoxicity, *Toxicol. Sci.*, 2015, **144**, 114-127.

31. J. Lan, N. Gou, C. Gao, M. He and A. Z. Gu, Comparative and mechanistic genotoxicity assessment of nanomaterials via a quantitative toxicogenomics approach across multiple species, *Environ. Sci. Technol.*, 2014, **48**, 12937-12945.

32. A. L. Alpatova, W. Shan, P. Babica, B. L. Upham, A. R. Rogensues, S. J. Masten, E. Drown, A. K. Mohanty, E. C. Alocilja and V. V. Tarabara, Single-walled carbon nanotubes dispersed in aqueous media via non-covalent functionalization: Effect of dispersant on the stability, cytotoxicity, and epigenetic toxicity of nanotube suspensions, *Water Res.*, 2010, **44**, 505-520.

33. X. Deng, F. Wu, Z. Liu, M. Luo, L. Li, Q. Ni, Z. Jiao, M. Wu and Y. Liu, The splenic toxicity of water soluble multi-walled carbon nanotubes in mice, *Carbon*, 2009, **47**, 1421-1428.

34. R. Klaper, D. Arndt, K. Setyowati, J. Chen and F. Goetz, Functionalization impacts the effects of carbon nanotubes on the immune system of rainbow trout, *Oncorhynchus mykiss*, *Aquat. Toxicol.*, 2010, **100**, 211-217.

35. S. Koyama, Y. A. Kim, T. Hayashi, K. Takeuchi, C. Fujii, N. Kuroiwa, H. Koyama, T. Tsukahara and M. Endo, In vivo immunological toxicity in mice of carbon nanotubes with impurities, *Carbon*, 2009, **47**, 1365-1372.

36. M. Ema, A. Matsuda, N. Kobayashi, M. Naya and J. Nakanishi, Evaluation of dermal and eye irritation and skin sensitization due to carbon nanotubes, *Regul. Toxicol. Pharmacol.*, 2011, **61**, 276-281.

37. F. Zhang, N. Wang, J. Kong, J. Dai, F. Chang, G. Feng and S. Bi, Multi-walled carbon nanotubes decrease lactate dehydrogenase activity in enzymatic reaction, *Bioelectrochemistry (Amsterdam, Netherlands)*, 2011, **82**, 74-78.

38. M. M. Alloy and A. P. Roberts, Effects of suspended multi-walled carbon nanotubes on daphnid growth and reproduction, *Ecotox. Environ. Safe.*, 2011, **74**, 1839-1843.

39. A. Helland, P. Wick, A. Koehler, K. Schmid and C. Som, Reviewing the environmental and human health knowledge base of carbon nanotubes, *Cienc. Saude. Coletiva.*, 2008, **13**, 441-452.

40. A. D. Ostrowski, T. Martin, J. Conti, I. Hurt and B. H. Harthorn, Nanotoxicology: characterizing the scientific literature, 2000-2007, *J. Nanopart. Res.*, 2009, **11**, 251-257.

41. S. Lanone, P. Andujar, A. Kermanizadeh and J. Boczkowski, Determinants of carbon nanotube toxicity, *Adv. Drug Deliv. Rev.*, 2013, **65**, 2063-2069.

42. C. D. Vecitis, K. R. Zodrow, S. Kang and M. Elimelech, Electronic-structure-dependent bacterial cytotoxicity of single-walled carbon nanotubes, *ACS Nano*, 2010, **4**, 5471-5479.

43. X. Wang, N. D. Mansukhani, L. M. Guiney, J. H. Lee, R. B. Li, B. B. Sun, Y. P. Liao, C. H. Chang, Z. X. Ji, T. Xia, M. C. Hersam and A. E. Nel, Toxicological profiling of highly purified metallic and semiconducting single-walled carbon nanotubes in the rodent lung and *E. coli*, *ACS Nano*, 2016, **10**, 6008-6019.

44. L. Berdjeb, E. Pelletier, J. Pellerin, J. P. Gagne and K. Lemarchand, Contrasting responses of marine bacterial strains exposed to carboxylated single-walled carbon nanotubes, *Aquat. Toxicol.*, 2013, **144**, 230-241.

45. M. Ema, H. Takehara, M. Naya, H. Kataura, K. Fujita and K. Honda, Length effects of single-walled carbon nanotubes on pulmonary toxicity after intratracheal instillation in rats, *J. Toxicol. Sci.*, 2017, **42**, 367-378.

46. D. F. Rodrigues, D. P. Jaisi and M. Elimelech, Toxicity of functionalized single-walled carbon nanotubes on soil microbial communities: implications for nutrient cycling in soil, *Environ. Sci. Technol.*, 2013, **47**, 625-633.

47. D. Fourches, D. Pu, C. Tassa, R. Weissleder, S. Y. Shaw, R. J. Mumper and A. Tropsha, Quantitative nanostructure-activity relationship modeling, *ACS Nano*, 2010, **4**, 5703-5712.

48. National Research Council, *Guide for the Care and Use of Laboratory Animals, 8th edition*, National Academies Press, Washington, DC, 2011.

49. N. A. Virani, C. Davis, P. McKernan, P. Hauser, R. E. Hurst, J. Slaton, R. P. Silvy, D. E. Resasco and R. G. Harrison, Phosphatidylserine targeted single-walled carbon nanotubes for photothermal ablation of bladder cancer, *Nanotechnology*, 2018, **29**.

50. A. Kavosi, S. Hosseini Ghale Noei, S. Madani, S. Khalighfard, S. Khodayari, H. Khodayari, M. Mirzaei, M. R. Kalhori, M. Yavarian, A. M. Alizadeh and M. Falahati, The toxicity and therapeutic effects of single-and multi-wall carbon nanotubes on mice breast cancer, *Sci. Rep.*, 2018, **8**, 8375.

51. D. Krewski, D. Acosta, Jr., M. Andersen, H. Anderson, J. C. Bailar, 3rd, K. Boekelheide, R. Brent, G. Charnley, V. G. Cheung, S. Green, Jr., K. T. Kelsey, N. I. Kerkvliet, A. A. Li, L. McCray, O. Meyer, R. D. Patterson, W. Pennie, R. A. Scala, G. M. Solomon, M. Stephens, J. Yager and L. Zeise, Toxicity testing in the 21st century: a vision and a strategy, *J. Toxicol. Environ. Health B*, 2010, **13**, 51-138.

52. D. Fourches, D. Pu and A. Tropsha, Exploring quantitative nanostructure-activity relationships (QNAR) modeling as a tool for predicting biological effects of manufactured nanoparticles, *Comb. Chem. High Throughput Screen.*, 2011, **14**, 217-225.

53. C. W. Schmidt, TOX 21: new dimensions of toxicity testing, *Environ. Health Perspect.*, 2009, **117**, A348-353.

54. A. Onnis-Hayden, H. Weng, M. He, S. Hansen, V. Ilyin, K. Lewis and A. Z. Gu, Prokaryotic real-time gene expression profiling for toxicity assessment, *Environ. Sci. Technol.*, 2009, **43**, 4574-4581.

55. J. Lan, N. Gou, S. M. Rahman, C. Gao, M. He and A. Z. Gu, A Quantitative toxicogenomics assay for high-throughput and mechanistic genotoxicity assessment and screening of environmental pollutants, *Environ. Sci. Technol.*, 2016, **50**, 3202-3214.

56. J. Lan, M. Hu, C. Gao, A. Alshawabkeh and A. Z. Gu, Toxicity assessment of 4-methyl-1-cyclohexanemethanol and its metabolites in response to a recent chemical spill in West Virginia, USA, *Environ. Sci. Technol.*, 2015, **49**, 6284-6293.

57. J. Lan, S. M. Rahman, N. Gou, T. Jiang, M. J. Plewa, A. Alshawabkeh and A. Z. Gu, Genotoxicity assessment of drinking water disinfection byproducts by dna damage and repair pathway profiling analysis, *Environ. Sci. Technol.*, 2018, **52**, 6565-6575.

58. K. Fujita, M. Fukuda, H. Fukui, M. Horie, S. Endoh, K. Uchida, M. Shichiri, Y. Morimoto, A. Ogami and H. Iwahashi, Intratracheal instillation of single-wall carbon nanotubes in the rat lung induces time-dependent changes in gene expression, *Nanotoxicology*, 2015, **9**, 290-301.

59. X. N. Cai, R. Ramalingam, H. S. Wong, J. P. Cheng, P. Ajuh, S. H. Cheng and Y. W. Lam, Characterization of carbon nanotube protein corona by using quantitative proteomics, *Nanomed-Nanotechnol*, 2013, **9**, 583-593.

60. Z. Q. Lin, L. Ma, Z. G. X, H. S. Zhang and B. C. Lin, A comparative study of lung toxicity in rats induced by three types of nanomaterials, *Nanoscale Res. Lett.*, 2013, **8**.

61. J. H. Shannahan, J. M. Brown, R. Chen, P. C. Ke, X. Y. Lai, S. Mitra and F. A. Witzmann, Comparison of nanotube-protein corona composition in cell culture media, *Small*, 2013, **9**, 2171-2181.

62. B. L. Blazer-Yost, A. Banga, A. Amos, E. Chernoff, X. Y. Lai, C. Li, S. Mitra and F. A. Witzmann, Effect of carbon nanoparticles on renal epithelial cell structure, barrier function, and protein expression, *Nanotoxicology*, 2011, **5**, 354-371.

63. W. T. Liu, M. Y. Bien, K. J. Chuang, T. Y. Chang, T. Jones, K. BeruBe, G. Lalev, D. H. Tsai, H. C. Chuang, T. J. Cheng and T. C. R. T.-C. Grp, Physicochemical and biological characterization of single-walled and double-walled carbon nanotubes in biological media, *J. Hazard. Mater.*, 2014, **280**, 216-225.

64. B. C. Lin, H. S. Zhang, Z. Q. Lin, Y. J. Fang, L. Tian, H. L. Yang, J. Yan, H. L. Liu, W. Zhang and Z. G. Xi, Studies of single-walled carbon nanotubes-induced hepatotoxicity by NMR-based metabonomics of rat blood plasma and liver extracts, *Nanoscale Res. Lett.*, 2013, **8**.

65. E. J. Park, Y. S. Hong, B. S. Lee, C. Yoon, U. Jeong and Y. Kim, Single-walled carbon nanotubes disturbed the immune and metabolic regulation function 13-weeks after a single intratracheal instillation, *Environ. Res.*, 2016, **148**, 184-195.

66. J. Sui, Y. Q. Zhang, C. Y. Li, Y. Y. Fu, S. M. Ma, M. Tang, L. H. Yin, Y. P. Pu and G. Y. Liang, Metabolic characteristics in serum of rats intratracheally instilled with multi-walled carbon nanotubes (MWCNT), *J. Nanosci. Nanotechno.*, 2017, **17**, 9236-9243.

67. R. H. Wang, C. Mikoryak, S. Y. Li, D. Bushdiecker, I. H. Musselman, P. Pantano and R. K. Draper, Cytotoxicity screening of single-walled carbon nanotubes: detection and removal of cytotoxic contaminants from carboxylated carbon nanotubes, *Mol. Pharmaceut.*, 2011, **8**, 1351-1361.

68. A. Nikitin, H. Ogasawara, D. Mann, R. Denecke, Z. Zhang, H. Dai, K. Cho and A. Nilsson, Hydrogenation of single-walled carbon nanotubes, *Phys. Rev. Lett.*, 2005, **95**, 225507.

69. C. A. Rodrigues-Pousada, T. Nevitt, R. Menezes, D. Azevedo, J. Pereira and C. Amaral, Yeast activator proteins and stress response: an overview, *FEBS Lett.*, 2004, **567**, 80-85.

70. X. D. Liu, P. C. C. Liu, N. Santoro and D. J. Thiele, Conservation of a stress response: human heat shock transcription factors functionally substitute for yeast HSF, *EMBO J.*, 1997, **16**, 6466-6477.

71. F. Estruch, Stress-controlled transcription factors, stress-induced genes and stress tolerance in budding yeast, *FEMS Microbiol. Rev.*, 2000, **24**, 469-486.

72. K. Yagi, Applications of whole-cell bacterial sensors in biotechnology and environmental science, *Appl. Microbiol. Biotechnol.*, 2007, **73**, 1251-1258.

73. S. Daunert, G. Barrett, J. S. Feliciano, R. S. Shetty, S. Shrestha and W. Smith-Spencer, Genetically engineered whole-cell sensing systems: coupling biological recognition with reporter genes.(Statistical Data Included), *Chem. Rev.*, 2000, **100**, 2705.

74. E. Z. Ron, Biosensing environmental pollution, *Curr. Opin. Biotech.,* 2007, **18**, 252-256.

75. W. K. Huh, J. V. Falvo, L. C. Gerke, A. S. Carroll, R. W. Howson, J. S. Weissman and E. K. O'Shea, Global analysis of protein localization in budding yeast, *Nature*, 2003, **425**, 686-691.

76. S. T. O'Connor, J. Lan, M. North, A. Loguinov, L. Zhang, M. T. Smith, A. Z. Gu and C. Vulpe, Genome-wide functional and stress response profiling reveals toxic mechanism and genes required for tolerance to benzo[a]pyrene in *S. cerevisiae*, *Front. Genet.*, 2012, **3**, 316.

77. S. M. Hohmann, Willem H., *Yeast Stress Responses*, Springer Berlin Heidelberg, 2003.

78. A. P. Gasch, P. T. Spellman, C. M. Kao, O. Carmel-Harel, M. B. Eisen, G. Storz, D. Botstein and P. O. Brown, Genomic expression programs in the response of yeast cells to environmental changes, *Mol. Biol. Cell*, 2000, **11**, 4241-4257.

79. A. Lucau-Danila, G. Lelandais, Z. Kozovska, V. Tanty, T. Delaveau, F. Devaux and C. Jacq, Early expression of yeast genes affected by chemical stress, *Mol. Cell Biol.*, 2005, **25**, 1860-1868.

80. M. Salamone, J. Heddle, E. Stuart and M. Katz, Towards an improved micronucleus test: studies on 3 model agents, mitomycin C, cyclophosphamide and dimethylbenzanthracene, *Mutat. Res.*, 1980, **74**, 347-356.

81. C. Godon, G. Lagniel, J. Lee, J. M. Buhler, S. Kieffer, M. Perrot, H. Boucherie, M. B. Toledano and J. Labarre, The H2O2 stimulon in Saccharomyces cerevisiae, *J. Biol. Chem.*, 1998, **273**, 22480-22489.

82. L. U. Ling, K. B. Tan, H. Lin and G. N. Chiu, The role of reactive oxygen species and autophagy in safingol-induced cell death, *Cell Death Dis.*, 2011, **2**, e129.

83. H. Wang and J. A. Joseph, Quantifying cellular oxidative stress by dichlorofluorescein assay using microplate reader, *Free Radic. Biol. Med.*, 1999, **27**, 612-616.

84. E. J. Petersen, C. Hirsch, J. T. Elliott, H. F. Krug, L. Aengenheister, A. T. Arif, A. Bogni, A. Kinsner-Ovaskainen, S. May, T. Walser, P. Wick and M. Roesslein, Cause-and-effect analysis as a tool to improve the reproducibility of nanobioassays: four case studies, *Chem. Res. Toxicol.*, 2019, **In Press**.

85. B. M. Dhawan A., Pandey A.K., Parmar D., in *ITRC: ThE SCGE/ Comet Assay Protocol*, 2009, vol. 1077, pp. 1-10.

86. A. I. Saeed, N. K. Bhagabati, J. C. Braisted, W. Liang, V. Sharov, E. A. Howe, J. Li, M. Thiagarajan, J. A. White and J. Quackenbush, TM4 microarray software suite, *Method. Enzymol.*, 2006, **411**, 134-193.

87. A. Subramanian, P. Tamayo, V. K. Mootha, S. Mukherjee, B. L. Ebert, M. A. Gillette, A. Paulovich, S. L. Pomeroy, T. R. Golub, E. S. Lander and J. P. Mesirov, Gene set enrichment analysis: a knowledge-based approach for

interpreting genome-wide expression profiles, *Proc. Natl. Acad. Sci. U.S.A.*, 2005, **102**, 15545-15550.

88. J. Wang, Q. Huang, Z. P. Liu, Y. Wang, L. Y. Wu, L. Chen and X. S. Zhang, NOA: a novel Network Ontology Analysis method, *Nucleic Acids Res.*, 2011, **39**, e87.

89. L. E. Haswell, S. Corke, I. Verrastro, A. Baxter, A. Banerjee, J. Adamson, T. Jaunky, C. Proctor, M. Gaça and E. Minet, In vitro RNA-seq-based toxicogenomics assessment shows reduced biological effect of tobacco heating products when compared to cigarette smoke, *Sci. Rep.*, 2018, **8**, 1145-1145.

90. S. Ishihara, C. J. O'Kelly, T. Tanaka, H. Kataura, J. Labuta, Y. Shingaya, T. Nakayama, T. Ohsawa, T. Nakanishi and T. M. Swager, Metallic versus semiconducting SWCNT chemiresistors: a case for separated SWCNTs wrapped by a metallosupramolecular polymer, *ACS Appl. Mater. Inter.*, 2017, **9**, 38062-38067.

91. B. Gigliotti, B. Sakizzie, D. S. Bethune, R. M. Shelby and J. N. Cha, Sequence-independent helical wrapping of single-walled carbon nanotubes by long genomic DNA, *Nano Lett.*, 2006, **6**, 159-164.

92. X. Pu, Z. Wang and J. E. Klaunig, Alkaline comet assay for assessing DNA damage in individual cells, *Curr. Protoc. Toxicol.*, 2015, **65**, 3.12.1-3.12.11.

93. M. H. Lin, T. S. Hsu, P. M. Yang, M. Y. Tsai, T. P. Perng and L. Y. Lin, Comparison of organic and inorganic germanium compounds in cellular radiosensitivity and preparation of germanium nanoparticles as a radiosensitizer, *Int. J. Radiat. Biol.*, 2009, **85**, 214-226.

94. S. K. Manna, S. Sarkar, J. Barr, K. Wise, E. V. Barrera, O. Jejelowo, A. C. Rice-Ficht and G. T. Ramesh, Single-walled carbon nanotube induces oxidative stress and activates nuclear transcription factor-kappa B in human keratinocytes, *Nano Lett.*, 2005, **5**, 1676-1684.

95. A. Nel, T. Xia, L. Madler and N. Li, Toxic potential of materials at the nanolevel, *Science (New York, N.Y.)*, 2006, **311**, 622-627.

96. A. K. Patlolla, P. K. Patra, M. Flountan and P. B. Tchounwou, Cytogenetic evaluation of functionalized single-walled carbon nanotube in mice bone marrow cells, *Environ. Toxicol.*, 2016, **31**, 1091-1102.

97. F. A. Girardi, G. E. Bruch, C. S. Peixoto, L. Dal Bosco, S. K. Sahoo, C. O. F. Goncalves, A. P. Santos, C. A. Furtado, C. Fantini and D. M. Barros, Toxicity of single-wall carbon nanotubes functionalized with polyethylene glycol in zebrafish (*Danio rerio*) embryos, *J. Appl. Toxicol.*, 2017, **37**, 214-221.

98. H. L. Karlsson, The comet assay in nanotoxicology research, *Anal. Bioanal. Chem.*, 2010, **398**, 651-666.

99. Z. Magdolenova, D. Bilanicova, G. Pojana, L. M. Fjellsbo, A. Hudecova, K. Hasplova, A. Marcomini and M. Dusinska, Impact of agglomeration and different dispersions of titanium dioxide nanoparticles on the human related in vitro cytotoxicity and genotoxicity (vol 14, pg 455, 2012), *J. Environ. Monitor.*, 2012, **14**, 3306-3306.

100. H. Yang, C. Liu, D. F. Yang, H. S. Zhang and Z. G. Xi, Comparative study of cytotoxicity, oxidative stress and genotoxicity induced by four typical

nanomaterials: the role of particle size, shape and composition, *J. Appl. Toxicol.*, 2009, **29**, 69-78.

101. D. Pantarotto, J. P. Briand, M. Prato and A. Bianco, Translocation of bioactive peptides across cell membranes by carbon nanotubes, *Chem. Commun.*, 2004, 16-17.

102. V. Raffa, G. Ciofani, O. Vittorio, C. Riggio and A. Cuschieri, Physicochemical properties affecting cellular uptake of carbon nanotubes, *Nanomedicine-UK*, 2010, **5**, 89-97.

103. X. H. Shi, A. von dem Bussche, R. H. Hurt, A. B. Kane and H. J. Gao, Cell entry of one-dimensional nanomaterials occurs by tip recognition and rotation, *Nat. Nanotechnol.*, 2011, **6**, 714-719.

104. N. W. S. Kam and H. J. Dai, Carbon nanotubes as intracellular protein transporters: Generality and biological functionality, *J. Am. Chem. Soc.*, 2005, **127**, 6021-6026.

105. P. Cherukuri, S. M. Bachilo, S. H. Litovsky and R. B. Weisman, Near-infrared fluorescence microscopy of single-walled carbon nanotubes in phagocytic cells, *J. Am. Chem. Soc.*, 2004, **126**, 15638-15639.

106. R. Foldbjerg, E. S. Irving, J. Wang, K. Thorsen, D. S. Sutherland, H. Autrupa and C. Beer, The toxic effects of single-walled carbon nanotubes are linked to the phagocytic ability of cells, *Toxicol. Res.*, 2014, **3**, 228-241.

107. X. J. Cui, B. Wan, Y. Yang, X. M. Ren and L. H. Guo, Length effects on the dynamic process of cellular uptake and exocytosis of single-walled carbon nanotubes in murine macrophage cells, *Sci. Rep.*, 2017, **7**.

108. B. M. Rotoli, O. Bussolati, A. Barilli, P. P. Zanello, M. G. Bianchi, A. Magrini, A. Pietroiusti, A. Bergamaschi and E. Bergamaschi, Airway barrier dysfunction induced by exposure to carbon nanotubes in vitro: which role for fiber length?, *Hum. Exp. Toxicol.*, 2009, **28**, 361-368.

109. A. C. W. Leung, S. Hrapovic, E. Lam, Y. L. Liu, K. B. Male, K. A. Mahmoud and J. H. T. Luong, Characteristics and properties of carboxylated cellulose nanocrystals prepared from a novel one-step procedure, *Small*, 2011, **7**, 302-305.

110. K. B. Male, A. C. W. Leung, J. Montes, A. Kamen and J. H. T. Luong, Probing inhibitory effects of nanocrystalline cellulose: inhibition versus surface charge, *Nanoscale*, 2012, **4**, 1373-1379.

111. K. A. Mahmoud, K. B. Male, S. Hrapovic and J. H. T. Luong, Cellulose nanocrystal/gold nanoparticle composite as a matrix for enzyme immobilization, *ACS Appl. Mater. Inter.*, 2009, **1**, 1383-1386.

112. W. R. Yang, P. Thordarson, J. J. Gooding, S. P. Ringer and F. Braet, Carbon nanotubes for biological and biomedical applications, *Nanotechnology*, 2007, **18**.

113. D. Gutierrez-Praena, S. Pichardo, E. Sanchez, A. Grilo, A. M. Camean and A. Jos, Influence of carboxylic acid functionalization on the cytotoxic effects induced by single wall carbon nanotubes on human endothelial cells (HUVEC), *Toxicol. in Vitro*, 2011, **25**, 1883-1888.

114. L. C. Felix, J. D. Ede, D. A. Snell, T. M. Oliveira, Y. Martinez-Rubi, B. Simard, J. H. T. Luong and G. G. Goss, Physicochemical properties of functionalized carbon-based nanomaterials and their toxicity to fishes, *Carbon*, 2016, **104**, 78-89.

115. M. S. Strano, C. A. Dyke, M. L. Usrey, P. W. Barone, M. J. Allen, H. W. Shan, C. Kittrell, R. H. Hauge, J. M. Tour and R. E. Smalley, Electronic structure control of single-walled carbon nanotube functionalization, *Science (New York, N.Y.)*, 2003, **301**, 1519-1522.

116. S. Banerjee and S. S. Wong, Selective metallic tube reactivity in the solution-phase osmylation of single-walled carbon nanotubes, *J. Am. Chem. Soc.*, 2004, **126**, 2073-2081.

117. C. M. Yang, J. S. Park, K. H. An, S. C. Lim, K. Seo, B. Kim, K. A. Park, S. Han, C. Y. Park and Y. H. Lee, Selective removal of metallic single-walled carbon nanotubes with small diameters by using nitric and sulfuric acids, *J. Phys. Chem. B*, 2005, **109**, 19242-19248.

118. G. Y. Zhang, P. F. Qi, X. R. Wang, Y. R. Lu, X. L. Li, R. Tu, S. Bangsaruntip, D. Mann, L. Zhang and H. J. Dai, Selective etching of metallic carbon nanotubes by gas-phase reaction, *Science (New York, N.Y.)*, 2006, **314**, 974-977.

119. M. Kanungo, H. Lu, G. G. Malliaras and G. B. Blanchet, Suppression of metallic conductivity of single-walled carbon nanotubes by cycloaddition reactions, *Science (New York, N.Y.)*, 2009, **323**, 234-237.

120. A. Kongkanand, R. M. Dominguez and P. V. Kamat, Single wall carbon nanotube scaffolds for photoelectrochemical solar cells. Capture and transport of photogenerated electrons, *Nano Lett.*, 2007, **7**, 676-680.

121. A. Kongkanand and P. V. Kamat, Electron storage in single wall carbon nanotubes. Fermi level equilibration in semiconductor-SWCNT suspensions, *ACS Nano*, 2007, **1**, 13-21.